

# EFFECT OF ZIRCONIUM SILICATE CONTENT ON DIELECTRIC AND MECHANICAL PROPERTIES OF POLYURETHANE ELASTOMER

M.N.M. Zaharin<sup>1</sup>, K.Z. Ku Ahmad<sup>1\*</sup>, R.N. Othman<sup>1</sup>, R. Yahaya<sup>2</sup> and M.A. Tarawneh<sup>3</sup>

<sup>1</sup>Engineering Faculty, Universiti Pertahanan Nasional Malaysia, Malaysia.

<sup>2</sup>Science and Technology Research Institute of Defense (STRIDE), Malaysia.

<sup>3</sup>College of Science, Al-Hussein Bin Talal University, Ma'an, Jordan.

\*Corresponding Author's Email: kuzarina@upnm.edu.my

**Article History:** Received 14 December 2022; Revised 22 July 2023;  
Accepted 5 August 2023

©2023 M.N.M. Zaharin et al. Published by Penerbit Universiti Teknikal Malaysia Melaka. This is an open article under the CC-BY-NC-ND license (<https://creativecommons.org/licenses/by-nc-nd/4.0/>).

**ABSTRACT:** Polyurethane (PU) is an interesting polymer that possesses excellent high dielectric permittivity, low dielectric loss, and great flexibility, which makes it promising to be applied as a dielectric elastomer generator (DEG). However, enhancement in terms of dielectric permittivity is still necessary to ensure PU practicability in the industry. On the other hand, while holding the potential to considerably enhance polymer dielectric properties, the investigation of zirconium silicate ( $ZrSiO_4$ ) as a nanofiller for DE composites remains insufficient. In this paper,  $ZrSiO_4$  was incorporated with PU matrix to study the impact of  $ZrSiO_4$  nanofillers on PU composite dielectric, chemical, mechanical and morphology properties.  $ZrSiO_4$  nanofillers and PU matrix were synthesized through the melt-mixing method at various weight percentages (10 wt.%, 20 wt.%, 30 wt.%, 40 wt.%, and 50 wt.%). Fourier Transform Infrared Spectroscopy (FTIR) was used to investigate the chemical characteristic of the composite. The dielectric and mechanical characterization of the composites was also studied. The results from FTIR indicate that the  $ZrSiO_4$  nanofillers were successfully synthesized within the PU matrix. Other than that, at 50 wt.% of  $ZrSiO_4$ , the PU/  $ZrSiO_4$  recorded dielectric permittivity up to 12.07 (33.5% higher than pristine PU) while maintaining low dielectric loss and low conductivity. The ultimate tensile stress and elongation at the break of the PU composites were affected by the increment of  $ZrSiO_4$  contents but they still maintained excellent

mechanical attributes. These PU/ZrSiO<sub>4</sub> composites have the potential to be used as dielectric elastomers in the DEG application.

**KEYWORDS:** *Polyurethane, Dielectric elastomer, Zirconium Silicate, Electrical properties, Polymer matrix composites*

## 1.0 INTRODUCTION

DE is a type of electroactive polymer (EAP) that exhibits deformation with the presence of an electric field. It possesses superiorities such as lightweight, large deformation, high energy density, rapid response, and ease of processing [1]. It can convert electrical energy into mechanical energy, and vice versa, making it suitable to be applied as both an actuator and a generator. The capacitance of DE is changeable, by manipulating the dielectric permittivity and mechanical properties of the elastomer, as shown in Eq. 1. In that equation,  $\epsilon_0$  represents permittivity of free space,  $\epsilon_r$  represents dielectric permittivity of the material, A represents the elastomer surface area and z represents the elastomer thickness.

$$C = \epsilon_0 \epsilon_r \frac{A}{Z} \quad (1)$$

One of the applications of DE is a dielectric elastomer generator (DEG), where the elastomer converts the oscillating mechanical power into usable electrical energy, identical to piezoelectric energy harvesting concept [2]. The working principle of DEG is illustrated in Figure 1 and described in Table 1 [3]. Based on the working principle, it is understandable that the performance of DEG relies on the dielectric and mechanical properties of the elastomer. The DEG needs to possess high dielectric permittivity, and also high elongation at break in order to harvest high electrical energy. The net amount of harvested energy can be calculated using Eq. 2, where U represents the harvested energy, C represents the capacitance of the elastomer, V represents the induced voltage, and 1 and 2 represent the relaxed and stretched states, respectively.

$$U = \frac{1}{2} C_2 V_2^2 - \frac{1}{2} C_1 V_1^2 \quad (2)$$

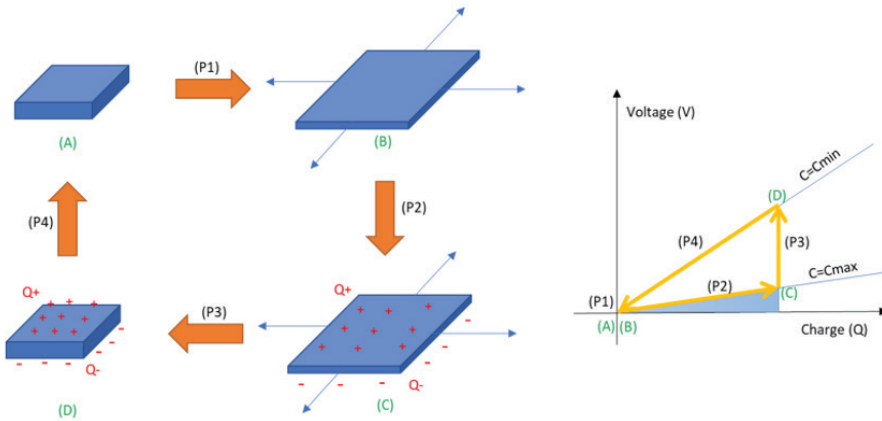


Figure 1: Illustration of DEG working principle [3]

Table 1: Description of DEG working principle [3]

Phase	Description
Phase 1 (P1)	In its initial state (A), the DEG is at rest with minimal capacitance. When subjected to external forces, it elongates and transitions to a stretched condition (B), resulting in maximum capacitance. There is an absence of charge on the DEG throughout this process.
Phase 2 (P2)	The deposition of charge, Q onto the electrodes causes the DEG to enter a charged state (C), characterized by the same capacitance as state (B). This stage is referred to as "priming," and it entails expending an amount of electrical energy to charge the device.
Phase 3 (P3)	While maintaining a constant charge on the DEG, the interaction between external forces and the elastic stress within the DEG counteracts the electrostatic charge. This process leads the DEG to revert to a state (D) characterized by the minimum capacitance, Cmin. Throughout this phase of generation, the external forces are transformed into electrostatic energy, which is then stored within the electric field of the DEG.
Phase 4 (P4)	Ultimately, the DEG is stabilized in a setup with the lowest capacitance and subsequently discharged, allowing for the extraction of the accumulated electrostatic energy. The overall quantity of generated electrical energy is determined by the disparity between the energy recouped during the discharging stage (P4) and the energy invested during the priming phase (P1).

The industry's capacity to use dielectric elastomers is still up for debate. Because of this, much research has been done over the years in the areas of material synthesis and optimization to create a DE that can meet the demands of the application. Researchers have often employed polymers with functionalized nanofiller to develop dielectric elastomers in order to accomplish specific objectives like high dielectric permittivity, superior breakdown strength, high actuation strain, etc. to various applications [4–6].

Of late, researchers have investigated a few methods to enhance the dielectric properties of DE. One of the methods is by incorporating ceramics fillers into the polymer matrix. This type of filler usually possesses high dielectric permittivity, which provides it with the ability to enhance the dielectric permittivity of the elastomer [7]. PU possesses high dielectric permittivity (~8) compare to other polymer such as acrylic or silicone rubber. However, the dielectric constant of PU elastomer is still necessary to ensure its practicality with industry applications [8].  $ZrSiO_4$  possesses high dielectric permittivity and it is abundant, making it a very cost-effective filler to be used to enhance polymer dielectric constant [9]. Despite its potential to significantly enhance polymer dielectric properties, the study of  $ZrSiO_4$  as a nanofiller for DE composites remains inadequate.

This study cooperates polyurethane (PU) matrix and zirconia silicate ( $ZrSiO_4$ ) to study the impact of  $ZrSiO_4$  on PU composite's properties. The preparation of PU/ $ZrSiO_4$  elastomer is described in this paper. The morphology, dielectric and mechanical properties of the PU/ $ZrSiO_4$  composite were investigated and analyzed for DEG application.

## **2.0 MATERIALS AND METHODS**

### **2.1 Materials**

The polyurethane (PU) granules, Zirconia (IV) Silicate ( $ZrSiO_4$ ) powder, and N-methyl-2-pyrrolidone (NMP) solvent were acquired from Sigma-Aldrich and used without further purification.

### **2.2 Preparation of the PU/ $ZrSiO_4$ composites**

The desired amount of  $ZrSiO_4$  nanoparticles (refer Table 2) was dispersed in 100 mL of NMP under sonication for 30 minutes, followed by adding 15g of PU and stirring the mixture mechanically for three hours at 150 rpm and 140°C. The mixture was poured into the glass mold and dried in an 80°C oven for 16 hours to eliminate all solvents. All the casted films then were removed from the mold. The films were then labelled as PU/  $ZrSiO_4$ -x, where x represents the weight percentage of  $ZrSiO_4$  nanoparticles.

Table 2: Amount of material used for each sample

Material	PU/ZrSiO <sub>4</sub> -10wt.%	PU/ZrSiO <sub>4</sub> -20wt.%	PU/ZrSiO <sub>4</sub> -30wt.%	PU/ZrSiO <sub>4</sub> -40wt.%	PU/ZrSiO <sub>4</sub> -50wt.%
PU	15g	15g	15g	15g	15g
ZrSiO <sub>4</sub>	1.5g	3g	4.5g	6g	7.5g

## 2.2 Characterization of Dielectric and Mechanical Properties

The composition of the PU, ZrSiO<sub>4</sub> and PU/ZrSiO<sub>4</sub>-50wt.% composite was characterized using FTIR at spectra between 4000 and 400 cm<sup>-1</sup>. The dielectric properties of the composites at different weight percentage of ZrSiO<sub>4</sub> were measured using an impedance analyzer (4294A, Agilent Technologies) in a frequency range of 30 Hz to 120 MHz at room temperature. The mechanical properties of the composite at different weight percentage of ZrSiO<sub>4</sub> were tested through a tensile test using Instron Universal Testing Machine according to ISO 37:2017 standard. The microstructural of PU/ZrSiO<sub>4</sub>-20wt.% and PU/ZrSiO<sub>4</sub>-50wt.% composites were characterized by high resolution field emission scanning electron microscope solutions (FESEM) (ZEISS GeminiSEM 500) and the elemental composition of both composites were mapped using Energy Dispersive X-Ray analysis (EDX).

## 3.0 RESULTS AND DISCUSSION

Figure 2 displays the FTIR spectra of PU, ZrSiO<sub>4</sub>, and PU/ZrSiO<sub>4</sub>-50wt.%. The absorbance observed around ~3335 cm<sup>-1</sup> aligns with the NH bond stretching, indicative of the urethane and urea groups. Additional distinctive bands are observed: around ~2900 cm<sup>-1</sup> corresponding to the alkane -CH stretching vibration, at 1174 cm<sup>-1</sup> reflecting the coupled C-N and C-O stretching vibrations, and at 1062 cm<sup>-1</sup> attributed to the symmetric stretching vibration of the ester C-O-C [10]. The spectral peaks at approximately ~431 and ~860 cm<sup>-1</sup>, evident in the ZrSiO<sub>4</sub> nanoparticles spectrum, can be associated with the asymmetric bending vibration and stretching vibration of Si-O-Si bonds, respectively. Furthermore, the peak at around ~650 cm<sup>-1</sup> is attributable to the Zr-O stretching vibrations [11], [12]. The presence of these bands in PU/ ZrSiO<sub>4</sub> composite indicates that the ZrSiO<sub>4</sub>

nanofillers are well dispersed in the PU matrix. All characteristic peaks are summarized in Table 3. There is no new band or peak presence in any composite samples, indicating there was no chemical reaction between PU and ZrSiO<sub>4</sub>.

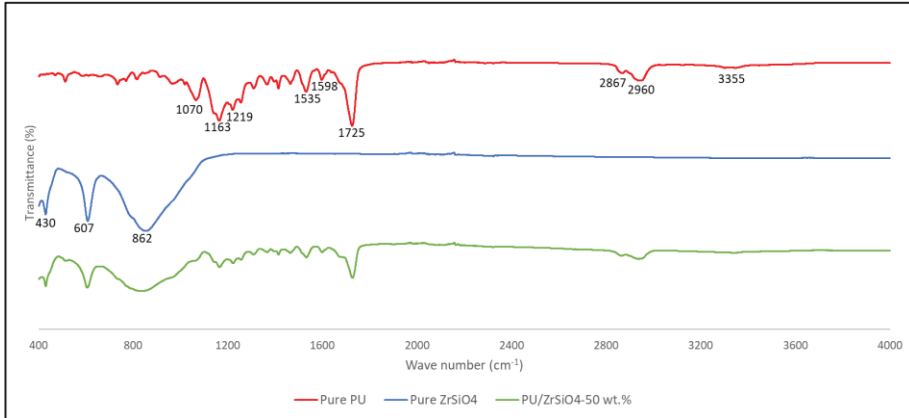


Figure 2: FTIR spectra of PU, ZrSiO<sub>4</sub> nanofillers and PU/ZrSiO<sub>4</sub>-50 wt.% composite

Table 3: FTIR characteristic band of PU, ZrSiO<sub>4</sub> and PU/ZrSiO<sub>4</sub>-50 wt.% composite

Frequency (cm-1)	Assignment
3050-3750	NH stretching vibration
2800-3000	CH stretching vibration: anti-symmetric and symmetric stretching vibration mode
1600-1800	Amide I: C=O stretching vibration
1500-1540	Amide II: C-N stretching
1200-1289	Amide III: in-plane N-H formation
1070-1074	C-N stretch
860	Stretching vibration of Si-O-Si
650	Zr-O stretching vibrations
431	Bending vibration of Si-O-Si

Figure 3 presents the dielectric constant of PU/ ZrSiO<sub>4</sub> composites at various weight percentages. The dielectric behavior of all composites suggests a frequency dependence of dielectric constant values, as the dielectric constant of all composites decreases with the increment of frequency. All composites displayed significant improvement in dielectric constant compared to conventional PU. The dielectric

constant of the composite increase with the increment of  $ZrSiO_4$  content, which similar trend was reported in other literature [13]. This increase in permittivity can be attributed to both the high permittivity of  $ZrSiO_4$  nanoparticles and the interfacial polarization between the nanoparticles and the PU matrix. As the  $ZrSiO_4$  content increases, the inherent high permittivity of the filler increasingly impacts the overall permittivity of the composites. Additionally, the dielectric constant of the filled elastomer is strongly influenced by interfacial polarization at the interface between PU and the  $ZrSiO_4$  nanoparticles, resulting in higher permittivity at low frequencies as  $ZrSiO_4$  loading concentration increases.

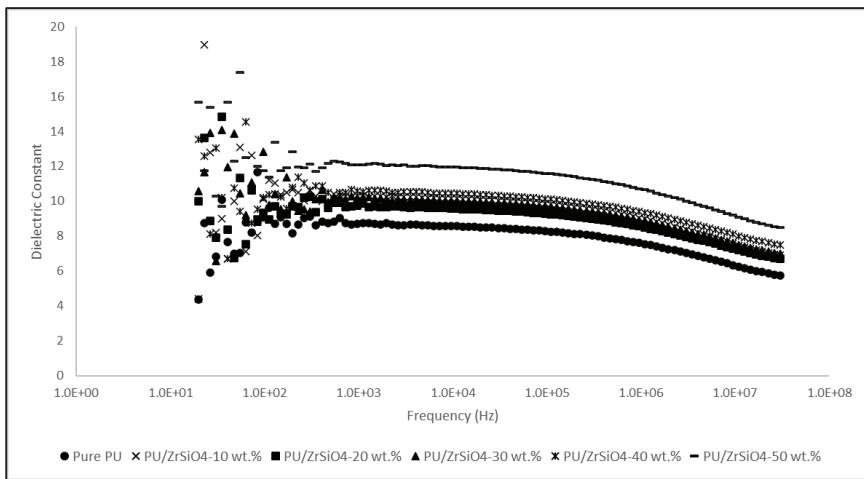


Figure 3: Dielectric permittivity of PU/ $ZrSiO_4$  composite at different weight percentages and frequencies

Figure 4 presents the dielectric losses for the PU/ $ZrSiO_4$  elastomer at different  $ZrSiO_4$  content. Notably, all composites exhibit lower dielectric loss values than the pure PU matrix, even at high  $ZrSiO_4$  loadings. The composite with 50 wt.% of  $ZrSiO_4$  demonstrated a particularly impressive dielectric loss of just 0.03 at 1 kHz, which is even lower than the dielectric loss of the pure PU matrix (0.05). This reduction in dielectric loss may be attributed to the insulative characteristics of ceramic materials found in  $ZrSiO_4$ , which limit current leakage and therefore influence the dielectric loss of the composite. Figure 5 displays the conductivity of the PU/ $ZrSiO_4$  composite at various weight percentages. The conductivity of the composites is lower than that of the pure PU elastomer. Increasing the content of  $ZrSiO_4$  did not

significantly impact the conductivity of the elastomer, as the conductivity remained low even at high  $ZrSiO_4$  content. This suggests that no conducting network was formed, indicating an insulation structure for this PU/  $ZrSiO_4$  composite film. The insulative characteristics of the ceramic materials found in  $ZrSiO_4$  are responsible for limiting current leakage and reducing the conductivity of the composite [14].

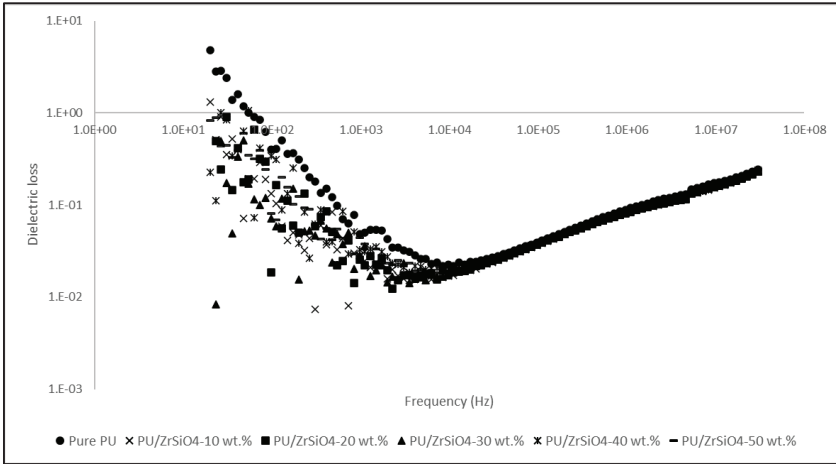


Figure 4: Dielectric loss of PU/  $ZrSiO_4$  composite at different weight percentages and frequencies

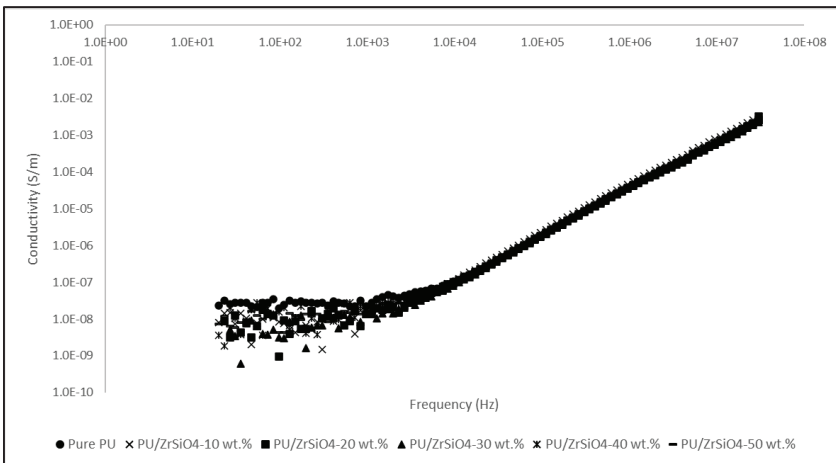


Figure 5: Conductivity of PU/ $ZrSiO_4$  composite at different weight percentages and frequencies



The mechanical properties of the elastomer have a vital influence on mechano-electrical energy conversion. Figure 6(a) shows the ultimate tensile stress of PU and PU/ZrSiO<sub>4</sub> composites. By increasing the ZrSiO<sub>4</sub> filler content to 20 wt.%, the tensile strength also increased due to particle enhancement. At 20 wt.% of ZrSiO<sub>4</sub>, the tensile stress of the composite reaches 6.74 MPa, which is a 122% increment. The enhancement in tensile strength is credited to the favorable interaction between the PU matrix and ZrSiO<sub>4</sub> fillers, which facilitates efficient stress transfer. The achievement of notable tensile strength relies significantly on the effective and consistent distribution of stress [15]. However, when the ZrSiO<sub>4</sub> content increases from 30 wt.% and above, the tensile strength decreases. This is due to the agglomeration of ZrSiO<sub>4</sub> filler within the PU matrix. It creates voids and acts as a flaw that limits tensile strength, as experienced in other literature [16]. On the other hand, the elongation at breaks of all elastomers was also investigated. Figure 6(b) shows the elongation at breaks of PU and PU/ZrSiO<sub>4</sub> composites. The findings demonstrate a decrease in elongation at break as the ZrSiO<sub>4</sub> content increases, signifying a transition in the PU matrix from a ductile material to a composite material with increased brittleness. However, even at 50 wt.% of ZrSiO<sub>4</sub> content, the composite still possesses high elongation at 587%.

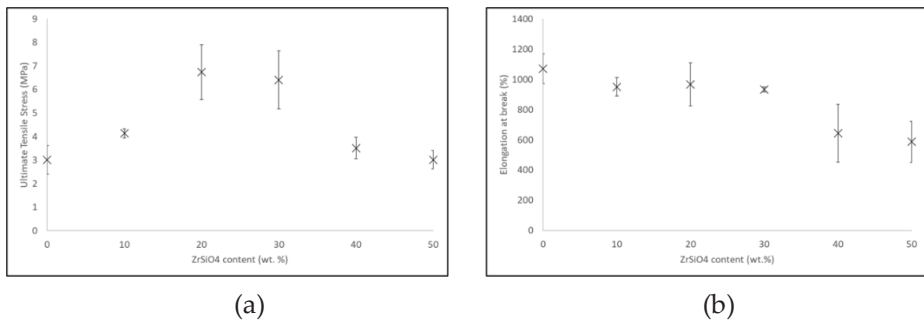


Figure 6 Mechanical characteristics of PU/ZrSiO<sub>4</sub> composites (a) ultimate tensile stress, (b) elongation at the break

The dispersion state of the ZrSiO<sub>4</sub> nanofillers within the PU matrix was further confirmed with FESEM images, as shown in Figure 8 (a-b). Figure 8(a) confirmed that the ZrSiO<sub>4</sub> nanofillers in PU/ZrSiO<sub>4</sub>-20 wt.% nanocomposite exhibit a more well-dispersed state where less agglomeration of nanofillers was observed, compared to PU/ZrSiO<sub>4</sub>-50 wt.% nanocomposite in figure 8(b). The agglomeration of nanofillers

provides a stress concentration effect and reduces the tensile strength of nanocomposite [17]. Other than that, the agglomeration nucleates voids and accelerates the propagation of internal cracks, causing the reduction of ductility, as reported in other literature [18]. These explained the differences in tensile strength and elongation capability between PU/ZrSiO<sub>4</sub>-20 wt.% and PU/ZrSiO<sub>4</sub>-50 wt.% nanocomposite. Further investigation using EDX analysis in Figure 9 (a-f) shows the dispersion of ZrSiO<sub>4</sub> nanofillers within the PU matrix. It is proven that the ZrSiO<sub>4</sub> nanofillers in PU/ZrSiO<sub>4</sub>-20 wt.% nanocomposite dispersed better compare to PU/ZrSiO<sub>4</sub>-20 wt.% nanocomposite, where agglomeration of nanofillers were presented.

#### 4.0 CONCLUSION

This study has successfully incorporated ZrSiO<sub>4</sub> with PU matrix, as demonstrated by the FTIR characterization. The presence of ZrSiO<sub>4</sub> helps in increasing the interfacial polarization with the PU matrix, which directly increases the dielectric permittivity of PU/ZrSiO<sub>4</sub> composites up to ~12 at 1 kHz (50% of enhancement compare to pure PU). Interestingly, the dielectric loss and the conductivity remain low (< 0.1), even at high ZrSiO<sub>4</sub> content. The mechanical characterization shows that the elongation of the composite deteriorates with the presence of ZrSiO<sub>4</sub> contents, but it still possesses high flexibility. The PU/ZrSiO<sub>4</sub> nanocomposite has promising potential for applications in the energy harvesting industry using elastomer, which requires high energy storage capability, low losses, and excellent flexibility.

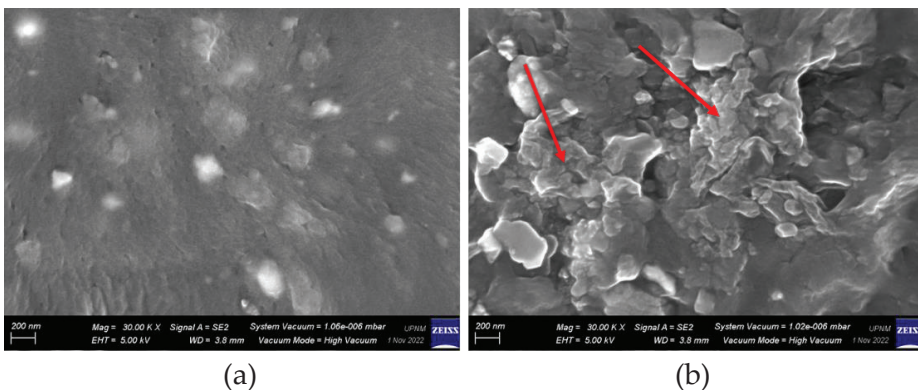


Figure 7 FESEM images of composite: (a) PU/ZrSiO<sub>4</sub>-20 wt.%; (b) PU/ZrSiO<sub>4</sub>-50 wt.% (red arrows indicate the location of ZrSiO<sub>4</sub> agglomerate).

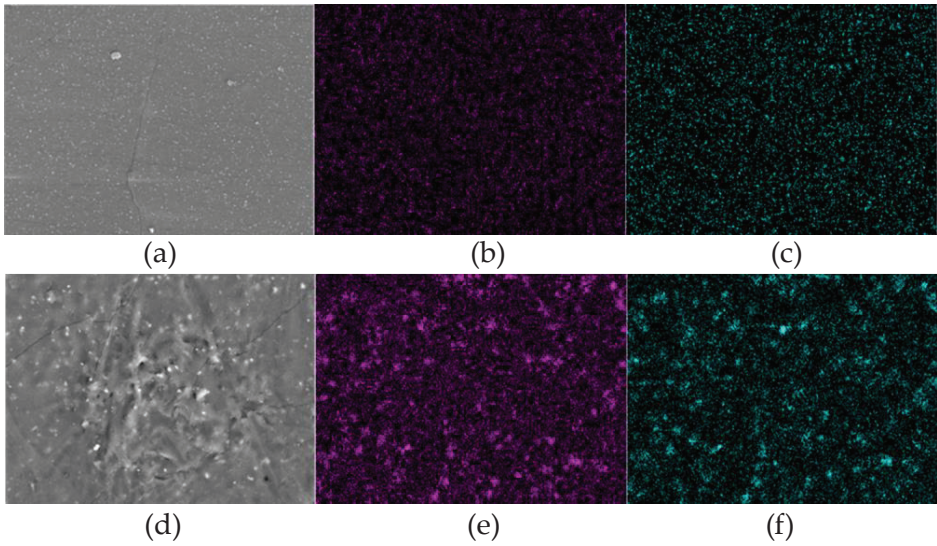


Figure 8 Nanocomposite EDX Mapping:

- (a) FESEM: PU/ZrSiO<sub>4</sub>-20 wt.% (b) Zr Mapping: PU/ZrSiO<sub>4</sub>-20 wt.%  
(c) Si Mapping: PU/ZrSiO<sub>4</sub>-20 wt.% (d) FESEM: PU/ZrSiO<sub>4</sub>-50 wt.%  
(e) Zr Mapping: PU/ZrSiO<sub>4</sub>-50 wt.% (f) Si Mapping: PU/ZrSiO<sub>4</sub>-50 wt.%

## ACKNOWLEDGMENTS

The authors would like to thank the Ministry of Higher Education Malaysia and the National Defense University Malaysia for providing financial support under FRGS/1/2020/TK0/UPNM/02/10.

## AUTHOR CONTRIBUTIONS

M.N.M. Zaharin: Conceptualization, Methodology, Data Curation Writing-Original Draft Preparation; K.Z. Ku Ahmad: Conceptualization, Methodology, Validation, Supervision, Writing-Reviewing and Editing; R. N. Othman: Data Curation, Writing-Original Draft Preparation, Writing-Reviewing and Editing; R. Yahaya: Validation, Supervision; M. A. Tarawneh: Validation, Supervision

## CONFLICTS OF INTEREST

The manuscript has not been published elsewhere and is not under consideration by other journals. All authors have approved the review, agree with its submission and declare no conflict of interest on the manuscript.

## REFERENCES

- [1] S. Gao, H. Zhao, N. Zhang, and J. Bai, "Enhanced Electromechanical Property of Silicone Elastomer Composites Containing TiO<sub>2</sub>@SiO<sub>2</sub> Core-Shell Nano-Architectures", *Polymers*, vol. 13, no. 3, p. 368, 2021.
- [2] M. Kamardan, A. Annuar, H. Zakaria, W. Ahmed, and W. Wan Hassan, "Development of Piezoelectric Harvesting System as An Alternative Renewable Energy for Automated Street Light in Malaysia", *Journal of Advanced Material Technology*, vol. 15, no. 2, 2021.
- [3] G. Moretti, S. Rosset, R. Vertechy, I. Anderson, and M. Fontana, "A Review of Dielectric Elastomer Generator Systems", *Advanced Intelligent System*, vol. 2, no. 10, pp. 1-30, 2020.
- [4] Y. Liu, L. Liu, Z. Zhang, and J. Leng, "Dielectric elastomer film actuators: characterization, experiment and analysis", *Smart Materials and Structure*, vol. 18, no. 9, pp. 1-10, 2009.
- [5] Z. Zhang, L. Liu, J. Fan, K. Yu, Y. Liu, L. Shi, and J. Leng, "New silicone dielectric elastomers with a high dielectric constant," in the 15th International Symposium on: Smart Structures and Materials & Nondestructive Evaluation and Health Monitoring, California, 2008, pp. 1-8.
- [6] K. K. Sadasivuni, D. Ponnamma, B. Kumar, M. Strankowski, R. Cardinaels, P. Moldenaers, S. Thomas, and T. Grohens, "Dielectric properties of modified graphene oxide filled polyurethane nanocomposites and its correlation with rheology", *Composite Science and Technology*, vol. 104, pp. 18-25, 2014.
- [7] W. Wan, J. Luo, C. Huang, J. Yang, Y. Feng, W. Yuan, Y. Ouyang, D. Chen, and T. Qiu, "Calcium copper titanate/polyurethane composite films with high dielectric constant, low dielectric loss and super flexibility", *Ceramic International*, vol. 44, no. 5, pp. 5086-5092, 2018.
- [8] P. Brochu and Q. Pei, "Advances in Dielectric Elastomers for Actuators and Artificial Muscles", *Macromolecular Rapid Communications*, vol. 31, no. 1, pp. 10-36, 2010.
- [9] J. Varghese, T. Joseph, and M. T. Sebastian, "ZrSiO<sub>4</sub> ceramics for microwave integrated circuit applications", *Materials Letters*, vol. 65, no. 7, pp. 1092-1094, 2011.
- [10] R. C. M. Dias, A. M. Góes, R. Serakides, E. Ayres, and R. L. Oréfice, "Porous biodegradable polyurethane nanocomposites: preparation, characterization, and biocompatibility tests", *Material Research*, vol. 13, no. 2, pp. 211-218, 2010.
- [11] Musyarofah, N. D. Lestari, R. Nurlaila, and N. F. Muwwoqor, "Synthesis of high-purity zircon, zirconia, and silica nanopowders from local zircon sand", *Ceramic International*, p. 38, 2019.

- [12] A. B. D. Nandiyanto, R. Oktiani, and R. Ragadhita, "How to Read and Interpret FTIR Spectroscopy of Organic Material", *Indonesia Journal of Science & Technology*, vol. 4, no. 1, p. 97, 2019.
- [13] J. Varghese, D. R. Nair, P. Mohanan, and M. T. Sebastian, "Dielectric, thermal and mechanical properties of zirconium silicate reinforced high density polyethylene composites for antenna applications", *Royal Society of Chemistry*, vol. 17, no. 22, pp. 14943–14950, 2015.
- [14] H. P. Palani Velayuda Shanmugasundram, E. Jayamani, and K. H. Soon, "A comprehensive review on dielectric composites: Classification of dielectric composites", *Renewable and Sustainable Energy Review*, vol. 157, pp. 1-24, 2022.
- [15] Y. Abbas and M. Anis-ur-Rehman, "Correlation of structure and dielectric response in Ce-doped double perovskite cobaltite", *Ceramic International*, vol. 48, no. 22, pp. 33389–33399, 2022.
- [16] R. S. Chen, S. Ahmad, M. H. A. Ghani, and M. N. Salleh, "Optimization of high filler loading on tensile properties of recycled HDPE/PET blends filled with rice husk," in the 2014 UKM FST Postgraduate Colloquium: Proceedings of the Universiti Kebangsaan Malaysia, Faculty of Science and Technology 2014 Postgraduate Colloquium, Selangor, 2014, pp. 46–51.
- [17] S. S. Chee and M. Jawaid, "The Effect of Bi-Functionalized MMT on Morphology, Thermal Stability, Dynamic Mechanical, and Tensile Properties of Epoxy/Organoclay Nanocomposites," *Polymers*, vol. 11, p. 1-18, 2019.
- [18] Y. Sun, Y. Zhao, J. Wu, X. Kai, Z. Zhang, Z. Fang, and C. Xia, "Effects of particulate agglomerated degree on deformation behaviors and mechanical properties of in-situ ZrB<sub>12</sub>/nanoparticles reinforced AA6016 matrix composites by finite element modeling", *Material Research Express*, vol. 7, no. 3, pp. 1-13, 2020.

